Journal of Nuclear Materials 414 (2011) 270–275

Contents lists available at ScienceDirect

Journal of Nuclear Materials

journal homepage: www.elsevier.com/locate/jnucmat

Presented at the NuMat 2010 Conference, 4–7 October 2010, Karlsruhe

Role of grain/phase boundary nature on the formation of hydrides in Zr–2.5%Nb alloy

K.V. Mani Krishna [a,*], D. Srivastava [a], G.K. Dey [a], V. Hiwarkar [b,1], I. Samajdar [b], S. Banerjee [a]

[a] Materials Science Division, Bhabha Atomic Research Centre, Trombay, Mumbai, India
[b] Department of Material Science and Engineering, IIT Bombay, Mumbai, India

ARTICLE INFO

Article history:
Received 29 October 2010
Accepted 1 April 2011
Available online 9 April 2011

ABSTRACT

Hydride formation in a fully recrystallized Zr–2.5%Nb alloy having equiaxed grains of α and β was studied. Primarily the electron back scatter diffraction (EBSD) technique was used for the characterization of the hydrides in conjunction with optical and transmission electron microscopy. Hydrides were found to have preferentially formed along the α/β interfaces. Microtexture measurements showed that the orientation relationship (OR) between α and δ-hydride phase was $(0\,0\,0\,1)_\alpha \parallel (1\,1\,1)_\delta$ and $[2\,\bar{1}\,1\,0]_\alpha \parallel [1\,1\,0]_\delta$. It was shown that the hydrides have higher preference to form along such α/β interfaces which have one of the low index planes of the β phase constituting the interface.

1. Introduction

Structural components made up of Zr based alloys are extensively used in the core of thermal nuclear reactors. However, formation of brittle hydride phase in these components is known to result in their property degradation, generically called as 'hydride embrittlement' [1,2]. In order to minimize such hydride induced degradation, it is desirable to develop optimized microstructures which can mitigate the problem of damage due to hydride formation to a reasonable extent [3]. Development of 'hydride embrittlement' resistant microstructures requires an understanding of the effect of microstructural parameters such as phase distribution, morphology on the formation of hydrides. In particular, knowledge of the role of second phase (β) on the precipitation behavior of the brittle hydrides is of great practical and scientific interest. Thorough understanding of the changes in hydride formation mechanism related to the presence of the second phase can help tailor the microstructures for a better 'hydride embrittlement' resistance.

Earlier studies have shown the grain boundaries to be preferential sites for the hydride formation, particularly under conditions of slow cooling relevant to nuclear reactors [4]. However, most of these observations are valid in case of hydride precipitation in the single phase Zr alloys such as Zircaloy-2 and Zircaloy-4 [4–12]. Some limited studies have shown that the α/β interfaces act as preferential sites for the precipitation of the hydrides in case of two phase Zr alloys such as Zr–2.5%Nb alloy [13–15]. However, such studies largely depended on the transmission electron microscopy (TEM) and/or optical microscopic examinations for the characterization of the hydrides and matrix microstructures. It was shown that OR (orientation relationship) derived from optical microscopy is different from that observed at a higher resolution in TEM [1,16]. On the other hand, observations from TEM have the limitations of statistical validity. In order to address these issues (of accurate determination of OR with improved statistics) and bring out the role of interfaces on the hydride precipitation, scanning electron microscope (SEM) based electron back scatter diffraction (EBSD) technique was employed in the present study for the characterization of the hydrides. The following important issues are being addressed in this present work:

- The role of α/β interfaces on the formation and growth of the hydrides.
- The reasons, if any, for the preference of hydrides for specific boundaries.

Zr–2.5%Nb alloy (two phase alloy containing hcp-α and bcc-β) has been selected as candidate material to meet the above objectives. A detailed characterization of the hydrided microstructures was carried out using the conventional techniques of optical and TEM along with extensive EBSD.

2. Experimental

The composition of the Zr–2.5%Nb alloy used in the present study is shown in Table 1. The alloy samples were subjected to 58% cold deformation by pilgering, followed by annealing at 700 °C for 14 days. The objective was to get equiaxed microstructure of the constituent phases, with beta grains at the tri-junctions of the alpha grains. Such microstructure is expected to have

* Corresponding author. Tel.: +91 22 25593289.
E-mail addresses: kvmani@barc.gov.in, kvmani@gmail.com (K.V. Mani Krishna).
[1] Present address: Crompton Greaves Ltd., Mumbai, India.

0022-3115/$ - see front matter © 2011 Elsevier B.V. All rights reserved.
doi:10.1016/j.jnucmat.2011.04.003

Table 1
Composition of the alloy used in the present study.

Element	Nb	O	H	N	Zr
Amount by weight	2.5%	1100 ppm	<5 ppm	30 ppm	Balance

significant amount of special interfaces (interfaces with specific misorientations) whose role on hydride formation is interesting to study.

Gaseous hydrogen charging was employed for hydrogenation of the samples. Samples were polished metallographically on all open faces (in order to increase surface area, and thus improve hydrogen absorption), followed by cleaning in acetone. Initially the sample chamber was evacuated to 1.0×10^{-8} bar pressure, and flushed with the hydrogen gas. Controlled amount of hydrogen was put into the system to achieve a pressure close to 1 bar. The sample was heated to 300 °C, and allowed to absorb the required amount of hydrogen. The difference in the initial and final hydrogen pressure was an indication of the amount of hydrogen absorbed by the sample. Samples were charged to nominal hydrogen levels of 200 and 300 ppm (by weight). The size of the specimens used for the study was approximately $10 \times 10 \times 4$ mm. The magnitude of the thickness of the sample ensured uniform hydrogen distribution under the experimental conditions used for hydrogen charging (A temperature of 300 °C for nearly 6 h followed by slow cooling). The stability of the base microstructure was assured during the hydrogenation, as the base microstructure was a fully recrystallized structure (annealed for 14 days at 700 °C) and is not expected to undergo any appreciable changes during hydrogenation as temperature (300 °C) and time (6 h) of hydrogenation were significantly low to induce any measurable changes in the base microstructure.

A Fei-3d® SEM mounted with a TSL-OIM® system was used for the EBSD measurements with a step size of 100 nm. Such a small step size ensured a reasonably good number of data points to be recorded inside each hydride plate. A number of EBSD scans spanning 100×300 μm^2 were performed on each sample covering a cumulative area close to 1 mm^2. This resulted in scanning several hundreds of alpha and beta grains, and tens of (close to 100) hydrides. The inherent difficulty in covering very large area in EBSD scans was due to the requirement of a very fine step size for successful indexing of the hydride phase. This was circumvented by scanning the sample at a number of locations through multiple scans. Samples for EBSD were prepared by the standard metallographic polishing followed by electro polishing using a solution consisting of 80% methanol and 20% perchloric acid at a temperature of −20 °C. A Technai 300® operated at 300 kV was used for TEM characterization.

3. Results

3.1. Distribution and nature of hydrides

Fig. 1 shows the distribution of the hydride phase in the Zr–2.5%Nb alloy sample with 300 ppm of hydrogen. The matrix microstructure essentially consisted of equiaxed grains of α phase with relatively large β grains at the tri-junctions of the α grains. Such a structure was the result of prolonged annealing at 700 °C for a period of 14 days following cold deformation. Grain sizes of the α phase were in the range of 5–10 μm. The β phase grain size ranged from 3 to 7 μm. The relative volume fractions of the α and β phases in the samples were 0.83 and 0.17 respectively. The hydrides in these samples were observed to be predominantly located along the interface boundaries of the α and β grains. The size of the hydrides was of the order of 5–10 μm along the length. The thickness of the hydrides on the other hand, ranged from 0.5 to 2 μm. A minor fraction of the hydrides were observed to have formed inside the α grains (intra-granular hydrides) and along the α/α grain boundaries as well. Morphology of the interface hydrides was evidently very different from that of the intra-granular hydrides. While the former followed the contours of the α/β interface, the latter have formed in sharp and straight needle like fashion along specific crystallographic planes. Though the formation of the hydrides was predominately along the α/β interface, their growth was always into adjacent α grain only. Interestingly, even though there are a considerable number of α/α grain boundaries present in these two phase samples, a majority of the hydrides have formed along the α/β interfaces only. No major differences in the crystallographic or morphological features of hydrides in samples with 200 and 300 ppm hydrogen were observed. Hence results from only 300 ppm samples are presented and are valid for samples with 200 ppm hydrogen as well.

EBSD has confirmed that the hydrides formed in these samples were of "δ" type which is an equilibrium hydride phase in the Zr–H system with a composition $ZrH_{1.5}$. Since the δ-hydride is the dominant hydride formed under reactor operation conditions (relatively slow cooling), the observations of the present study bear more practical significance. TEM characterization of the hydrided samples has further confirmed that the α/β interface is the most preferred site for the hydride formation in these samples, see Fig. 2. TEM also has shown that, though hydrides have formed along the α/β interface, they have grown into adjoining α grains only. Further, the δ and β interface was more sharper and showed relatively less strain contrast in comparison to the corresponding δ/α interface as can be observed from Fig. 2. The diffraction patterns recorded in the TEM also confirmed the hydrides to be equilibrium δ-hydride. Superimposition of the diffraction patterns from

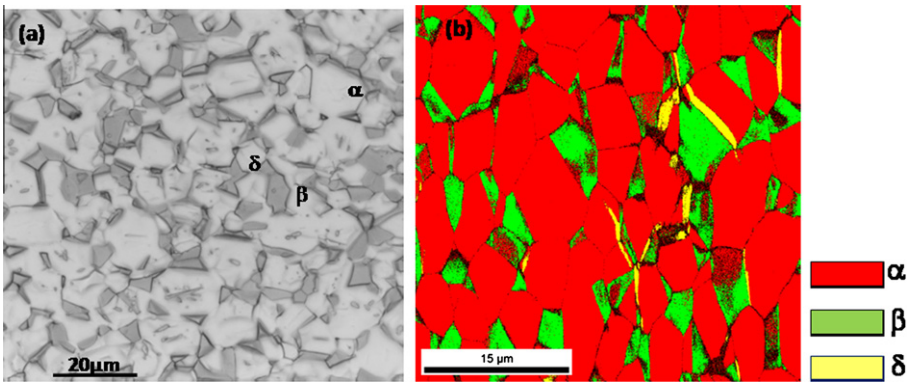

Fig. 1. (a) Optical and (b) EBSD micrographs showing the distribution of the hydrides in Zr–2.5%Nb alloy charged with 300 ppm (by weight) of hydrogen. In the optical micrograph light, gray and dark regions correspond respectively to α, β and δ-hydride phases.

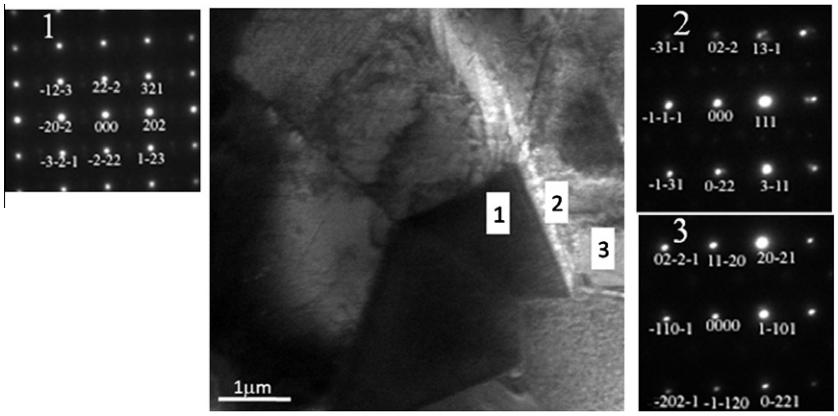

Fig. 2. TEM micrograph showing the presence of the hydride along the α/β interface. Diffraction patterns from the different regions (marked with the numbers) are superimposed. Electron diffraction from the respective phases was recorded using a selected area diffraction aperture. This has ensured the diffraction to be recorded from the intended phase only without the interference of the adjoining phases.

α, β and δ-hydride phases indicated that they are having OR with each other.

3.2. Microtexture of the hydrides

EBSD measurements of the orientations inside the hydride phase have indicated that even the largest hydrides (observed in this study), which were of nearly 10 μm in length, were having single orientation with an orientation spread not exceeding 2°. This is in contrast to the previous studies which have reported that most of the large hydrides which were visible under optical microscope were actually stacks of several hydride plates in succession [16,17]. The nature of the α/δ and β/δ interfaces are shown in terms of the respective misorientation distribution function (MODF) plots in the Fig. 3. An MODF plot is a graphical representation of the presence (or lack) of preference of grain/interface boundaries with reference to what is expected from a random distribution of boundaries [18]. MODF typically uses the angle/axis convention for the representation of the grain/interphase boundaries. The angle corresponds to the misorientation between the two crystals and axis corresponds to the vector about which one of the crystal needs to be rotated to match its lattice orientation with the other crystal. Similar to an ODF (Orientation distribution function), MODF is a distribution in three dimensional orientation space. Hence one can plot the MODF as a contour map in the constant intervals of misorientation angles about stereographic triangle representing the crystal axes. When the constituent phases of a microstructure exhibit orientation relationship with each other, one shall get higher intensity contours around the point representing the OR in the MODF. Thus an MODF facilitates an easy way to identify the OR between different phases. As can be seen from the Fig. 3a, there is a strong OR between the α-Zr and δ-hydride, as indicated by the maximum intensity value of 21 times to the random distribution. The observed OR corresponded to

$$(0\,0\,0\,1)_{\alpha} \parallel (1\,1\,1)_{\delta}$$

$$[2\,\bar{1}\,1\,0]_{\alpha} \parallel [1\,1\,0]_{\delta}$$

It may be emphasized that this OR was derived by analyzing a number of hydrides in a two phase zirconium alloy using the EBSD information (with higher statistical validity), and is in agreement with the previous studies based on TEM observations [1,14,15] and other EBSD based studies of single phase zirconium alloys [9–11]. The OR between the β phase and δ-hydride, on the other

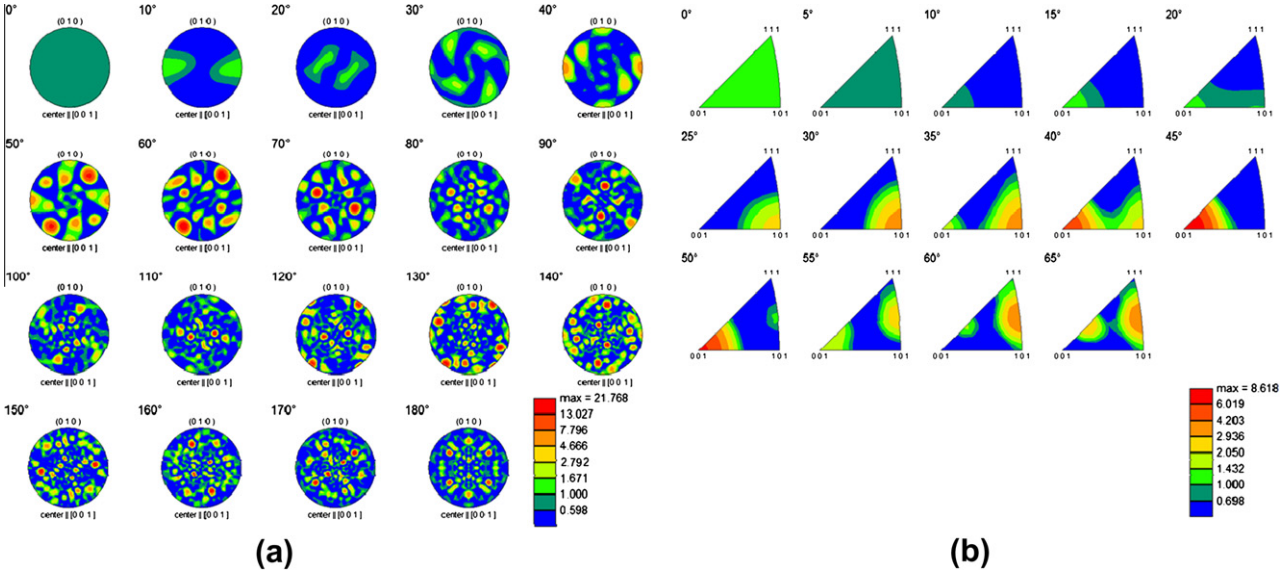

Fig. 3. (a) Misorientation distribution function plot (MODF) for the α and δ-hydride boundaries. (b) MODF for the β and δ-hydride boundaries.

hand, is not as strong, see Fig. 3b, maximum MODF intensity being close to 8 times to the random distribution. Analysis of individual interface hydrides has shown the presence of following OR (with considerable scatter of 20°) between the β and δ-hydride.

$(0\,1\,1)_{\beta} \parallel (1\,1\,1)_{\delta}$

$[1\,0\,0]_{\beta} \parallel [1\,1\,0]_{\delta}$

Since TEM as well as EBSD results have shown conclusively, that the hydride phase was growing only into the adjoining α grains but not into the β phase, existence of the OR between the δ-hydride and β phase is somewhat surprising.

The three phases i.e., α, *β* and δ-hydride have clear difference in their in-grain misorientation profiles. This is clearly shown in Fig. 4, which is a plot of grain average misorientation (GAM) distribution in the different phases. The GAM is a measure of extent of remnant plastic strain in the grains. Under the measurement conditions of the EBSD used in the present study, 0.3° of error in orientation measurement is to be expected, which can be taken as the cut off for the presence or absence of remnant plastic strain. The plot clearly shows that the GAM distribution of β phase is lowest and is close to machine error, indicating virtually strain free β grains. In contrast δ-hydride shows highest development in GAM suggesting towards accumulation of considerable plastic strain inside it. α phase on the other hand, showed GAM distribution intermediate to the former two phases. The present study thus provides a quantitative measure of strain partitioning between the various phases arising out of transformation strain caused by hydride precipitation. The observed strain partitioning could be attributed to selective partitioning of hydride transformation strains to α phase in preference to β phase. Since the formation of the $ZrH_{1.5}$ involves a volume expansion of 17%, considerable plastic strain is expected both in the hydride as well as the α grains into which it was growing. These observations, are in line with the TEM observations which indicated absence of any significant strain at the β/δ interface, Fig. 2.

3.3. Preference of hydrides for specific α/β interfaces

The results presented so far have unequivocally confirmed the formation of the hydrides preferentially along the α/β interfaces. However, in order to investigate if all of the α/β boundaries (characterized by their misorientation expressed in angle/axis pair) have equal probability of hydride formation, specific boundaries are superimposed on the EBSD-phase map as shown in Fig. 5. The blue lines in the figure indicate the Burger's boundaries, i.e., those α/β interfaces which have a misorientation corresponding to Burger's OR (45°@ $[2\,\bar{1}\,1\,0]_{\alpha}$ or 45°@ $[0\,0\,1]_{\beta}$) within a tolerance of 10°. EBSD analysis of the grain boundaries showed that the length fraction of such Burger's boundaries was 10% of the total boundary length which includes all of the α/β and α/α boundaries. Furthermore, among all of the α/β boundaries about 40% were observed to be of Burger's boundaries. If the hydrides have no specific preference to these Burger's boundaries, only 10% of the hydrides are expected along these interfaces. However, as shown in Fig. 5, nearly all of the hydrides are located along the Burger's boundaries only, indicating a strong preference of the hydrides to form along the α/β interfaces which follow Burger's OR. It is also interesting to note that not all the interfaces that were found to be following Burger's OR were having hydrides forming along them. This suggests that apart from misorientation between the α and *β* some additional factors govern the feasibility of hydride formation.

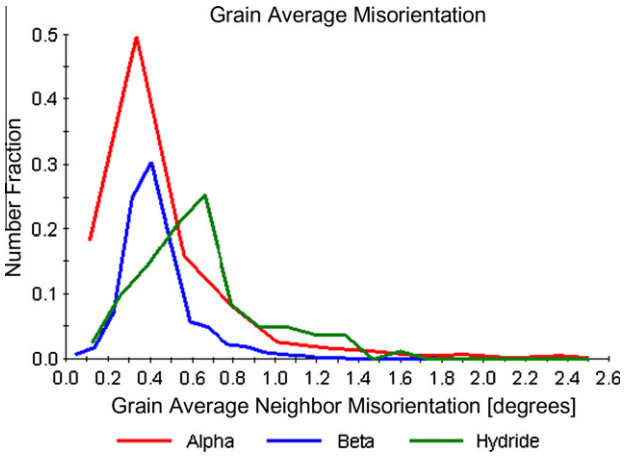

Fig. 4. Grain average misorientation (GAM) distribution in α, *β* and δ-hydride phases. Only the grains where hydrides were observed were considered for this plot. This is due to the fact that misorientation due to hydride formation can occur only in the grains adjacent to hydrides.

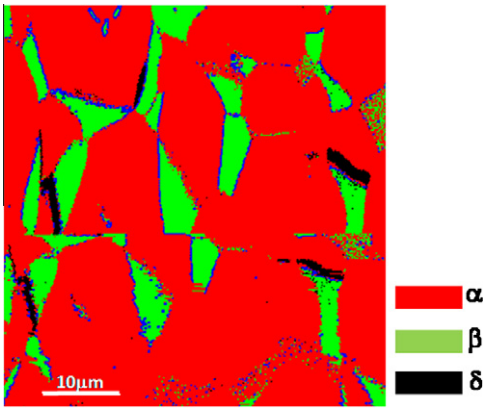

Fig. 5. Phase map showing the interface hydrides along with the α/β interfaces following the Burger's OR within a tolerance of 10° from the ideal Burger's OR (in blue). (For interpretation of the references to colour in this figure legend, the reader is referred to the web version of this article.)

Boundary trace analysis was performed on the interface hydrides to determine the interface plane on which δ-hydride was forming. In doing this analysis it was assumed that the observed interface plane was perpendicular to the plane of measurement, i.e., interface plane normal lied in the plane of the measurement. This assumption was necessitated because of 2-D nature of the EBSD measurement which does not allow knowing the tilt and twist nature of the boundary [18]. Even then, the information gained using such assumption can be useful in differentiating the hydride forming and non-forming boundaries to some qualitative extent. The results of the analysis, indicated that the hydrides were growing parallel to one of the low index planes of the β phase. $(1\,0\,0)_{\beta}$, $(1\,1\,0)_{\beta}$ were found to be the most commonly observed β planes onto which δ-hydrides were growing. Unlike in case of β and δ-hydride interfaces where in most cases they shared a low index plane (such as (0 0 1) or (1 1 0)) as the interface, the α/δ-hydride interface was found to be invariably a high index plane. In addition α/δ-hydride interface planes showed considerable scatter and no single dominant plane as a favored interface could be identified.

4. Discussion

Studies aiming at the understanding of the formation of the hydrides in Zirconium alloys have largely been driven by their immense practical relevance in controlling the damage due to

the hydride embrittlement. Most of such previous studies, however, have depended mainly on the optical and/or TEM techniques for the characterization of the hydrides [12–15]. With the advent of modern tool of EBSD, it is possible to revisit some of the previous observations to gain new insights into the phenomena governing the formation of hydrides [4,9–11]. In a recent study, extensive use of microtexture data obtained from EBSD, has been shown to give invaluable information on the role played by the special boundaries on the formation of the hydrides in case of single phase recrystallized Zircaloy-2 [4]. Investigation of the role played by the interfaces, if any, in case of two phase alloy systems on the formation of hydrides, naturally is a logical extension of such studies and thus becomes the motivation for the present study.

The main observations of the present study can be summarized as:

- Hydrides in the two phase Zr–2.5%Nb alloy in a completely recrystallized condition have formed primarily along α/β interfaces, with only a minor fraction of hydrides being along α/α grain boundaries.
- Though hydrides have a strong OR with the α phase into which they were growing, there was some apparent OR between the hydrides and β phase too.
- The majority of the hydrides were observed along those α/β interfaces which have a misorientation corresponding to Burger's OR. However, not all the α/β interfaces which are related by the Burger's OR are having the hydrides along them.
- Hydrides have grown on one of the low index planes of the β phase while their interface plane with the α phase appeared to be arbitrary, i.e., no set of low index planes could be identified as preferred interface planes.

Grain and/or phase boundaries are known to be some of the most potential sites for the heterogeneous nucleation of product phases [19,20]. Hence the observation of the α/β interfaces to be the preferred sites for the hydride formation is not surprising. However, formation of the hydrides along α/β interfaces in preference to α/α boundaries (which are also present in significant proportion) needs to be explained. The main reason attributed for the effectiveness of the grain boundaries as potential nucleation sites is their relatively higher energy. However, in the present study, experimental evidence shows the formation of hydrides along the α/β interfaces which are related by Burger's OR. Such interfaces are expected to be low energy interfaces, due to relatively higher atomic matching across the interface [21–23]. Hence the governing factors for the selection of α/β interfaces as preferred hydride nucleation sites have to be more than mere boundary/interface energy.

In general, precipitation of a secondary phase in a two phase system depends on relative concentration, amount and solid solubility of the constituent phases in addition to the nature and number of nucleation sites available for precipitation [19,24]. In this context, spatial distribution of the hydrogen in the sample can have an important role in determining the preferred sites of hydride formation. The hydrogen charging temperature used in the present study was 300 °C, which incidentally is also the operating temperature of the PHWR (pressurized heavy water reactor) reactors. At this temperature, the solid solubility of hydrogen in β and α phases are considerably different, hydrogen being more soluble in the β phase [25,26]. The hydrogen solubility data in the beta phase is available for composition of 20%Nb only [25]. There are no reports of any significant deviation of the hydrogen solubility in the beta phase as a function of the Nb content to the knowledge of the authors. Hence as a first approximation the hydrogen solubility of the beta phase observed in the present study (with a Nb content of approximately 13–14%) can be assumed to be equal or close to the beta phase with 20%Nb. A hydrogen solubility ratio of 9 between β-Zr (20%Nb) and α-Zr was reported [27]. Such a large variation in hydrogen solubility in the constituent phases leads to considerable hydrogen partitioning between the two phases at the hydrogenation temperature. In other words, selective accumulation of the hydrogen in β phase takes place. Considering the nominal level of 300 ppm of hydrogen used in the present study, and taking the solubility of hydrogen in α-Zr as 60 ppm (at 300 °C) [25,27], it can be shown that only 17% of the total hydrogen will be in α-Zr at the hydrogenation temperature. In contrast, as high as 83% of total hydrogen will be in β-Zr which constituted only 17% of the volume fraction of the microstructure used in the present study. When the sample is cooled, during which the hydride precipitation takes place, diffusion of hydrogen to the nearest potential nucleation site is expected to be the critical step [28]. Naturally, α/β interfaces happen to be the nearest interfaces for a majority of the hydrogen atoms due to higher concentration of the hydrogen in β grains. Furthermore, the diffusivity of the hydrogen in the β phase is much higher than that in the α phase [29]. The potential of the α/β interfaces for aiding the nucleation of hydride phase is further enhanced by the fact that the β grains observed in the present study are primarily located at tri-junctions of the α grains. It is a well known fact that the tri-junctions are one of the strongest heterogeneous nucleation sites for solid state phase transformations, like precipitation [19,24]. Since α phase does have some hydrogen dissolved in it at the temperature of hydrogenation, precipitation of hydrides along α/α grain boundaries is possible in a condition where there is no suitable α/β interface is present in the vicinity of the hydrogen atoms. This can explain the observation of a relatively small fraction of hydrides along α/α grain boundaries. In addition, since the hydrogenation temperature used in the present study is 300 °C and the level of hydrogen charging is up to 300 ppm, one would expect formation of hydride phase at the hydrogenation temperature, as the terminal solid solubility (TSS) of the alpha phase is only 60 ppm at this temperature. This also leads to formation of some hydrides along the α/α. However, it is to be noted that number fraction of such hydrides is low (see the Section 3.1) compared to the hydrides that formed along the α/β interfaces as the bulk of the hydrogen is concentrated in the β phase due to the hydrogen partitioning arising out of wide variation in solubilities of α and β phase for hydrogen.

The present study has also shown that, though nucleation of the hydrides has taken place along the α/β interface, their growth occured only into the adjoining α grains. Although a detailed thermodynamic analysis is beyond the scope of the present study, previous works [30–33] suggest that the thermodynamic driving force for the $\alpha \rightarrow ZrH_{1.5}$ transformation to be stronger than that of the $\beta \rightarrow ZrH_{1.5}$ transformation. This is a consequence of a higher affinity of hydrogen to Zr than to Nb which is present in significant amount in β phase [25]. This implies that the presence of a OR between the β and δ-hydride cannot be due to $\beta \rightarrow ZrH_{1.5}$ transformation. The observed OR between the interface δ-hydride and β is in fact a consequence of the fact that most of the α/β interfaces have Burger's OR and δ has stronger OR with the α phase.

In summary, the present study has shown the important role played by the nature of interfaces on the precipitation of hydrides making use of microtextural information obtained from EBSD. It has provided the quantitative measure of strain partitioning during the formation of hydrides at the α/β interfaces. Hydride precipitation was shown to depend on the level of hydrogen partitioning at the hydrogenation temperature and availability of suitable β interfaces (low index planes of β phase) which are conducive for the growth of hydride phase into the adjoining α phase.

References

[1] D.O. Northwood, U. Kosasih, Int. Metall. Rev. 28 (1983) 92–121.
[2] M.P. Puls, Nucl. Eng. Des. 171 (1997) 137–148.
[3] I. Batra, R. Singh, P. Sengupta, B. Maji, K. Madangopal, K.M. Krishna, R. Tewari, G. Dey, J. Nucl. Mater. 389 (2009) 500–503.
[4] K.V.M. Krishna, A. Sain, I. Samajdar, G.K. Dey, D. Srivastava, S. Neogy, R. Tewari, S. Banerjee, Acta Mater. 54 (2006) 4665–4675.
[5] P. Vizcaino, A.D. Banchik, J.P. Abriata, J. Mater. Sci. 42 (2007) 6633–6637.
[6] H.C. Chu, S.K. Wu, R. Kuo, J. Nucl. Mater. 373 (2008) 319–327.
[7] Y. Shinohara, H. Abe, T. Iwai, N. Sekimura, T. Kido, H. Yamamoto, T. Taguchi, J. Nucl. Sci. Technol. 46 (2009) 564–571.
[8] Sakai, Tadamiti, Kakuma, Tsutom, Nagai, Trans. Jpn. Inst. Met. 14 (1973) 194–198.
[9] K. Une, K. Nogita, S. Ishimoto, K. Ogata, J. Nucl. Sci. Technol. 41 (2004) 731–740.
[10] K. Une, S. Ishimoto, J. Nucl. Mater. 389 (2009) 436–442.
[11] N.A.P.K. Kumar, J.A. Szpunar, Z. He, J. Nucl. Mater. 403 (2010) 101–107.
[12] J. Bradbrook, G. Lorimer, N. Ridley, J. Nucl. Mater. 42 (1972) 142–160.
[13] V. Perovic, G. Weatherly, J. Nucl. Mater. 126 (1984) 160–169.
[14] V. Perovic, G. Weatherly, S. MacEwen, M. Leger, Acta Metall. Mater. 40 (1992) 363–372.
[15] V. Perovic, G. Weatherly, C. Simpson, Acta Metall. 31 (1983) 1381–1391.
[16] V. Perovic, G. Weatherly, C. Simpson, Scripta Metall. 16 (1982) 409–412.
[17] R.N. Singh, P. Stahle, L. Banks-Sills, M. Ristinmaa, S. Banerjee, Defect Diffusion Forum 279 (2008) 105–110.
[18] V. Randle, O. Engler, Introduction to Texture Analysis Microtexture and Orientation Mapping, Taylor and Francis Limited, 2003.
[19] D.A. Porter, K.E. Sterling, Phase Transformation in Metals and Alloys, Nelson Thornes, 2001.
[20] B. Verlinden, J. Driver, I. Samajdar, Thermo-Mechanical Processing of Metallic Materials, Elsevier, 2007.
[21] V. Hiwarkar, S. Sahoo, K. Mani Krishna, I. Samajdar, G. Dey, D. Sri- vastav, R. Tewari, S. Banarjee, R. Doherty, Acta Mater. 57 (2009) 5812–5821.
[22] D. Srivastava, G.K. Dey, S. Banerjee, Metall. Mater. Trans. A 26 (1995) 2707–2718.
[23] D. Srivastava, K. Madangopal, S. Banerjee, S. Ranganathan, Acta Metall. Mater. 41 (1993) 3445–3454.
[24] R.D. Doherty, D.A. Hughes, F.J. Humphreys, J.J. Jonas, D.J. Jensen, M. Kassner, W.E. King, T.R. McNelley, H.J. McQueen, A.D. Rollett, Mater. Sci. Eng. A: Struct. Mater.: Prop., Microstruct. Process. 238 (1997) 219–274.
[25] D. Khatamian, V.C. Ling, J. Alloys Compd. 253–254 (1997) 162–166.
[26] B. Skinner, R. Dutton, Hydrogen diffusivity in alpha–beta zirconium alloys and its role in delayed hydride cracking, The Minerals, Metals and Materials Society, 1990.
[27] D. Khatamian, J. Alloys Compd. 293–295 (1999) 893–899.
[28] R. Tang, X. Yang, Int. J. Hydrogen Energy 34 (2009) 7269–7274.
[29] A. Aladjem, Diffusion Defect Data Pt. B: Solid State Phenom. 49–50 (1996) 281–329. Cited by (since 1996) 4.
[30] J. Wang, L. Wang, W. Chen, Q. Huang, J. Shen, J. Nucl. Mater. 409 (2011) 47–52.
[31] F. Guillermet, Armando, Z. Metallkd./Mater. Res. Adv. Tech. 82 (1991) 478–487.
[32] E. Knigsberger, G. Eriksson, W.A. Oates, J. Alloys Compd. 299 (2000) 148–152.
[33] J.F. Smith, Bull. Alloy Phase Diagrams 4 (1983) 39–46.